J. KSIAM Vol.22, No.4, 217–239, 2018 http://dx.doi.org/10.12941/jksiam.2018.22.217

INFLUENCE OF HALL CURRENT AND HEAT SOURCE ON MHD FLOW OF A ROTATING FLUID IN A PARALLEL POROUS PLATE CHANNEL

M. VENKATESWARLU [1†], G. UPENDER REDDY [2], AND D. VENKATA LAKSHMI [3]

[1]DEPARTMENT OF MATHEMATICS, V. R. SIDDHARTHA ENGINEERING COLLEGE, KRISHNA (DIST), ANDHRA PRADESH, INDIA, PIN: 520 007
E-mail address: mvsr2010@gmail.com

[2]DEPARTMENT OF MATHEMATICS, MAHATMA GANDHI UNIVERSITY, ANNEPARTHY, NALGONDA (DIST), TELANGANA STATE, INDIA, PIN: 508 254
E-mail address: upendermathsmgu@gmail.com

[3]DEPARTMENT OF MATHEMATICS, BAPATLA WOMEN'S ENGINEERING COLLEGE, BAPATLA, GUNTUR (DIST), ANDHRA PRADESH, INDIA, PIN: 522 102
E-mail address: himaja96@gmail.com

ABSTRACT. This paper examined the MHD and thermal behavior of unsteady mixed convection flow of a rotating fluid in a porous parallel plate channel in the presence of Hall current and heat source. The exact solutions of the concentration, energy and momentum equations are obtained. The influence of each governing parameter on non dimensional velocity, temperature, concentration, skin friction coefficient, rate of heat transfer and rate of mass transfer at the porous parallel plate channel surfaces is discussed. During the course of numerical computation, it is observed that as Hall current parameter and Soret number at the porous channel surfaces increases, the primary and secondary velocity profiles are increases while the primary and secondary skin friction coefficients are increases at the cold wall and decreases at the heated wall. In particular, it is noticed that a reverse trend in case of heat source parameter.

1. INTRODUCTION

Investigation of MHD flows in a rotating system is of great importance because of its wide range industrial applications in rotating MHD generators, turbo machines, rotating drum-type separators for liquid metal MHD applications, electromagnetic stirring of liquid metal in continuous casting machines. It is observed that the Coriolis force is stronger than inertia and viscous forces whereas Coriolis and magnetic forces are comparable in magnitude. In addition, the Coriolis force induces a secondary flow in the flow field. Given the importance of this study, unsteady MHD mixed convection flow in a rotating system has been investigated by several researchers considering different aspects of the problem. Sharma and Chaudhary [1]

Received by the editors April 10 2018; Accepted December 6 2018; Published online December 21 2018.
2000 *Mathematics Subject Classification.* 85A30, 35K05, 81V70, 76SXX.
Key words and phrases. MHD, Hall current, Heat absorption, Soret effect, Parallel plate channel.
† Corresponding author.

presented the hydromagnetic unsteady mixed convection and mass transfer flow past a vertical porous plate immersed in a porous medium in presence of Hall current. Salem and Abd El-Aziz [2] investigated the effect of Hall currents and chemical reaction on hydromagnetic flow of a stretching vertical surface with internal heat generation or absorption. Venkateswarlu and Venkata Lakshmi [3] presented the Dufour and chemical reaction effects on unsteady MHD flow of a viscous fluid in a parallel porous plate channel under the influence of slip condition. Turkyilmazoglu [4] presented the exact solutions for the incompressible, viscous and magneto-hydrodynamic fluid of a porous rotating disk flow with Hall current. Khan et al. [5] discussed the mass transport on chemicalized fourth-grade fluid propagating peristaltically through a curved channel with magnetic effects. Ellahi et al. [6] considered the effects of Hall and ion slip on MHD peristaltic flow of Jeffrey fluid in a non-uniform rectangular duct. Venkateswarlu and Venkata Lakshmi [7] reported the thermal diffusion, Hall current and chemical reaction effects on unsteady MHD natural convective flow past a vertical plate. Sarkar and Seth [8] discussed the unsteady hydromagnetic natural convection flow past a vertical plate with time dependent free stream through a porous medium in the presence of Hall current, rotation and heat absorption. Tripathi et al. [9] presented the effects of transverse magnetic field on the peristaltic transport of viscoelastic fluid with Jeffrey model in a finite length channel. Jha and Apere et al. [10] studied the Hall and ion-slip on unsteady MHD Couette flow in a rotating system with suction and injection. Venkateswarlu et al. [11] discussed the effects of chemical reaction and heat generation on MHD boundary layer flow of a moving vertical plate with suction and dissipation. Jha and Oni [12] presented an exact solution to the electromagnetic natural convection flow in a vertical micro-channel with joule heating.

The convection problem in porous media has important applications in geothermal reservoirs, geothermal energy extractions, coal gasification, iron blast furnaces, ground water hydrology, wall cooled catalytic reactors, energy efficient drying processes, solar power collectors, cooling of nuclear fuel in shipping flasks, cooling of electronic equipments and natural convection in earths crust. Venkateswarlu et al. [13] studied the diffusion-thermo effects on MHD flow past an infinite vertical porous plate in the presence of radiation and chemical reaction. Bhatti et al. [14] presented the mathematical modeling of heat and mass transfer effects on MHD peristaltic propulsion of two-phase flow through a Darcy-Brinkman-Forchheimer porous medium. Ellahi et al. [15] discussed the combine porous and magnetic effect on some fundamental motions of Newtonian fluids over an infinite plate. Venkateswarlu and Makinde [16] presented the unsteady MHD slip flow with radiative heat and mass transfer over an inclined plate embedded in a porous medium. Das et al. [17] considered the Hall effects on unsteady rotating MHD flow through porous channel with variable pressure gradient. Recently, Venkateswarlu et al. [18, 19, 20] reported the Soret and Dufour effects on radiative MHD slip flow of a viscous fluid in a parallel porous plate channel under the influence of heat absorption and chemical reaction.

The following strategy is pursued in the rest of the paper. Section two presents the formation of the problem. The analytical solutions are presented in section three. Results are discussed in section four and finally section five provides a conclusion of the paper.

2. Formation of the Problem

Consider the non linear, unsteady hydromagnetic natural convection flow of a viscous, incompressible, electrically conducting, heat absorbing and rotating fluid between two infinite parallel porous walls $y = 0$ and $y = a$ in the presence of a uniform transverse magnetic field of strength B_0 that is applied parallel to $y-$ axis taking Hall current into account. Select the coordinate system in such way that $x-$ axis is along the length of the plate in the horizontal direction, $y-$ axis is along the channel width in the vertical direction and $z-$ axis perpendicular to $xy-$ plane. Both the fluid and channel rotate in unison with a uniform angular velocity Ω about $y-$ axis. Fluid flow within the channel is induced due to uniform pressure gradient applied along $x-$ direction as well as the movement of upper wall $y = a$ with uniform velocity u_0 in the same direction. Initially i.e. at $y = 0$, both the fluid and plate are at rest and maintained at uniform temperature $T = T_0$ and uniform concentration $C = C_0$. At $y = a$, temperature of the plate is raised to uniform temperature $T = T_1$. Also, species concentration at the surface of the plate is raised to uniform species concentration $C = C_1$. Physical model of the problem is presented in Fig.1. Since channel walls are of infinite extent in $x-$ and $z-$ directions, all physical quantities, except pressure gradient depend on y and t only. It is assumed that the induced magnetic field produced by fluid motion is negligible in comparison to the applied one.

Keeping in view of the above assumptions, the governing equations for non linear, unsteady, hydromagnetic mixed convection flow of a viscous, incompressible, electrically conducting and heat absorbing fluid in a in a rotating system taking Hall current and Soret effects into account are presented in the following form

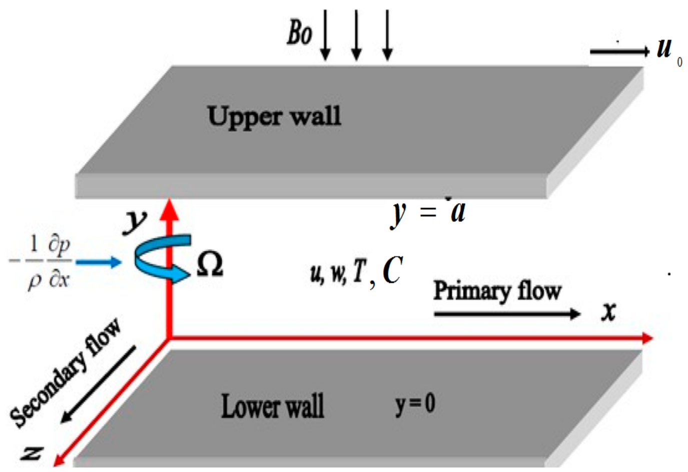

FIGURE 1. Geometry of the problem.

Continuity equation:

$$\frac{\partial v}{\partial y} = 0 \tag{2.1}$$

Momentum equations:

$$\frac{\partial u}{\partial t} + 2\Omega w = -\frac{1}{\rho}\frac{\partial p}{\partial x} + \nu\frac{\partial^2 u}{\partial y^2} - \frac{\sigma B_0^2}{\rho}\left[\frac{u+mw}{1+m^2}\right] + g\beta_T(T-T_0) + g\beta_C(C-C_0) - \frac{\nu}{K_1}u \tag{2.2}$$

$$\frac{\partial w}{\partial t} - 2\Omega u = -\frac{1}{\rho}\frac{\partial p}{\partial z} + \nu\frac{\partial^2 w}{\partial y^2} - \frac{\sigma B_0^2}{\rho}\left[\frac{mu-w}{1+m^2}\right] - \frac{\nu}{K_1}w \tag{2.3}$$

Energy equation:

$$\frac{\partial T}{\partial t} = \frac{k_T}{\rho c_p}\frac{\partial^2 T}{\partial y^2} - \frac{Q_0}{\rho c_p}(T-T_0) \tag{2.4}$$

Concentration equation:

$$\frac{\partial C}{\partial t} = D_m\frac{\partial^2 C}{\partial y^2} + \frac{D_m k_T}{T_m}\frac{\partial^2 T}{\partial y^2} \tag{2.5}$$

where $m = \omega_e\tau_e$ – Hall current parameter, ω_e – cyclotron frequency, τ_e – electron collision time, u – fluid velocity in x – direction, v – fluid velocity in y – direction, w – fluid velocity in z – direction, p – fluid pressure, g – acceleration due to gravity, ρ – fluid density, β_T – coefficient of thermal expansion, β_C – coefficient of concentration expansion, t – time, K_1 – permeability of porous medium, B_0 – magnetic induction, T – fluid temperature, T_0 – temperature at the cold wall, k_T – thermal diffusivity of the fluid, Q_0 – dimensional heat source parameter, C – species concentration in the fluid, C_0 – concentration at the cold wall, σ – fluid electrical conductivity, c_p – specific heat at constant pressure, D_m – chemical molecular diffusivity, T_m – mean fluid temperature and ν – kinematic viscosity of the fluid respectively.

Assuming that no slipping occurs between the plate and fluid, the corresponding initial and boundary conditions of the system of partial differential equations are given below

$$\begin{aligned} &u = 0,\ w = 0,\ T = T_0,\ C = C_0 \text{ at } y = 0 \\ &u = u_0,\ w = 0,\ T = T_1 + \epsilon(T_1 - T_o)\exp(int), \\ &C = C_1 + \epsilon(C_1 - C_0)\exp(int) \text{ at } y = a \end{aligned} \tag{2.6}$$

where T_1 - fluid temperature at the heated plate, C_1 - species concentration at the heated plate, n - frequency of oscillation and $\epsilon << 1$ is a very small positive constant.

For purely an oscillatory flow, we take the pressure gradient terms $-\frac{1}{\rho}\frac{\partial p}{\partial x}$ and $-\frac{1}{\rho}\frac{\partial p}{\partial z}$ are of the form (see, Makinde et al. [21])

$$\frac{\partial p}{\partial x} = -\frac{\sigma B_0^2 u_0}{(1+m^2)} \tag{2.7}$$

$$\frac{\partial p}{\partial z} = 2\Omega u_0\rho + \frac{\sigma B_0^2 m u_0}{(1+m^2)} \tag{2.8}$$

By substituting the equations (2.7) and (2.8) into the equations (2.2) and (2.3) we get

$$\frac{\partial u}{\partial t}+2\Omega w=\nu\frac{\partial^2 u}{\partial y^2}-\frac{\sigma B_0^2}{\rho}\left[\frac{u+mw-u_0}{1+m^2}\right]+g\beta_T(T-T_0)+g\beta_C(C-C_0)-\frac{\nu}{K_1}u \quad (2.9)$$

$$\frac{\partial w}{\partial t}-2\Omega(u-u_0)=\nu\frac{\partial^2 w}{\partial y^2}-\frac{\sigma B_0^2}{\rho}\left[\frac{mu_0+w-mu}{1+m^2}\right]-\frac{\nu}{K_1}w \quad (2.10)$$

We introduce the following non-dimensional variables

$$\eta=\frac{y}{a},U=\frac{a}{\nu}u,W=\frac{a}{\nu}w,\omega=\frac{a^2}{\nu}n,\tau=\frac{\nu}{a^2}t,\theta=\frac{T-T_0}{T_1-T_0},\phi=\frac{C-C_0}{C_1-C_0} \quad (2.11)$$

Equations (2.4), (2.5), (2.9) and (2.10) reduces to the following non-dimensional form

$$\frac{\partial U}{\partial \tau}+2K^2W=\frac{\partial^2 U}{\partial \eta^2}-\frac{M(U+mW-\lambda)}{1+m^2}+Gr\theta+Gm\phi-\frac{U}{K} \quad (2.12)$$

$$\frac{\partial W}{\partial \tau}-2K^2(U-\lambda)=\frac{\partial^2 W}{\partial \eta^2}-\frac{M(m\lambda+W-mU)}{1+m^2}-\frac{W}{K} \quad (2.13)$$

$$\frac{\partial \theta}{\partial \tau}=\frac{1}{Pr}\frac{\partial^2 \theta}{\partial \eta^2}-H\theta \quad (2.14)$$

$$\frac{\partial \phi}{\partial \tau}=\frac{1}{Sc}\frac{\partial^2 \phi}{\partial \eta^2}+Sr\frac{\partial^2 \theta}{\partial \eta^2} \quad (2.15)$$

Here $K^2=\frac{\Omega a^2}{\nu}$ is the rotation parameter, $M=\frac{\sigma B_0^2 a^2}{\rho\nu}$ is the magnetic parameter, $\lambda=\frac{u_0 a}{\nu}$ is the upper wall motion parameter, $K=\frac{K_1}{a^2}$ is the permeability parameter, $Gr=\frac{g\beta_T(T_1-T_0)a^3}{\nu^2}$ is the thermal buoyancy force, $Gm=\frac{g\beta_C(C_1-C_0)a^3}{\nu^2}$ is the concentration buoyancy force, $Pr=\frac{\rho c_p \nu}{k_T}$ is the Prandtl number, $H=\frac{Q_0 a^2}{\rho c_p \nu}$ is the heat source parameter, $Sc=\frac{\nu}{D_m}$ is the Schmidt number and $Sr=\frac{D_m k_T(T_1-T_0)}{T_m\nu(C_1-C_0)}$ is the Soret number respectively.

The corresponding initial and boundary conditions can be written as

$$\begin{aligned}&U=0,\ W=0,\ \theta=0,\ \phi=0 \ \text{ at } \eta=0\\ &U=\lambda,\ W=0,\ \theta=1+\epsilon\ \exp(i\omega\tau),\ \phi=1+\epsilon\ \exp(i\omega\tau) \text{ at } \eta=1\end{aligned} \quad (2.16)$$

Equations (2.12) and (2.13) can be written in compact form as follows

$$\frac{\partial \psi}{\partial \tau}-2iK^2(\psi-\lambda)=\frac{\partial^2 \psi}{\partial \eta^2}-\frac{M(\psi-\lambda)}{1+im}+Gr\theta+Gm\phi-\frac{\psi}{K} \quad (2.17)$$

The corresponding initial and boundary conditions in compact form can be written as

$$\begin{aligned}&\psi=0,\ \theta=0,\ \phi=0 \ \text{ at } \eta=0\\ &\psi=\lambda,\ \theta=1+\epsilon\ \exp(i\omega\tau),\ \phi=1+\epsilon\ \exp(i\omega\tau) \text{ at } \eta=1\end{aligned} \quad (2.18)$$

Given the velocity, temperature and concentration fields in the boundary layer, the shear stress τ_w, the heat flux q_w and mass flux j_w are obtained as

$$\tau_w = \mu\left[\frac{\partial\psi}{\partial y}\right] \tag{2.19}$$

$$q_w = -k_T\left[\frac{\partial T}{\partial y}\right] \tag{2.20}$$

$$j_w = -D_m\left[\frac{\partial C}{\partial y}\right] \tag{2.21}$$

In non-dimensional form the skin-friction coefficient Cf, heat transfer coefficient Nu and mass transfer coefficient Sh are defined as

$$Cf = \frac{\tau_w}{\rho(\frac{\nu}{a})^2} \tag{2.22}$$

$$Nu = \frac{aq_w}{k_T(T_1 - T_0)} \tag{2.23}$$

$$Sh = \frac{aj_w}{D_m(C_1 - C_0)} \tag{2.24}$$

Using non-dimensional variables in equation (2.11) and equations (2.19) to (2.21) into equations (2.22) to (2.24), we obtain the physical parameters

$$Cf = \left[\frac{\partial\psi}{\partial\eta}\right] \tag{2.25}$$

$$Nu = -\left[\frac{\partial\theta}{\partial\eta}\right] \tag{2.26}$$

$$Sh = -\left[\frac{\partial\phi}{\partial\eta}\right] \tag{2.27}$$

3. SOLUTION OF THE PROBLEM

Equations (2.14), (2.15) and (2.17) are coupled non-linear partial differential equations and these cannot be solved in closed form. So, we reduce these non-linear partial differential equations into a set of ordinary differential equations, which can be solved analytically. This can be done by assuming the trial solutions for the velocity, temperature and concentration of the fluid as(see, Adesanya and Makinde [22], Venkateswarlu and Venkata Lakshmi [23])

$$\psi(\eta,\tau) = \psi_0(\eta) + \epsilon\, exp(i\omega\tau)\psi_1(\eta) + 0(\epsilon^2) \tag{3.1}$$

$$\theta(\eta,\tau) = \theta_0(\eta) + \epsilon\, exp(i\omega\tau)\theta_1(\eta) + 0(\epsilon^2) \tag{3.2}$$

$$\phi(\eta,\tau) = \phi_0(\eta) + \epsilon\, exp(i\omega\tau)\phi_1(\eta) + 0(\epsilon^2) \tag{3.3}$$

Substituting equations (3.1) to (3.3) into equations(2.14), (2.15) and (2.17), then equating the harmonic and non-harmonic terms and neglecting the higher order terms of $0(\epsilon^2)$, we obtain

$$\psi_0^{''} - \Big[\frac{M}{1+im} + \frac{1}{K} - 2iK^2\Big]\psi_0 = -Gr\theta_0 - Gm\phi_0 - \left[\frac{M}{1+im} - 2iK^2\right]\lambda \tag{3.4}$$

$$\psi_1^{''} - \Big[\frac{M}{1+im} + \frac{1}{K} - 2iK^2 + i\omega\Big]\psi_1 = -Gr\theta_1 - Gm\phi_1 \tag{3.5}$$

$$\theta_0^{''} - PrH\,\theta_0 = 0 \tag{3.6}$$

$$\theta_1^{''} - Pr\,[H + i\omega]\theta_1 = 0 \tag{3.7}$$

$$\phi_0^{''} = -ScSr\theta_0^{''} \tag{3.8}$$

$$\phi_1^{''} - Sc\,i\,\omega\,\phi_1 = -ScSr\theta_1^{''} \tag{3.9}$$

where the prime denotes the ordinary differentiation with respect to η .
The corresponding initial and boundary conditions can be written as

$$\begin{array}{l} \psi_0 = 0,\ \psi_1 = 0,\ \theta_0 = 0, \theta_1 = 0, \phi_0 = 0,\ \phi_1 = 0, \text{ at } \eta = 0 \\ \psi_0 = \lambda,\ \psi_1 = 0,\ \theta_0 = 1,\ \theta_1 = 1, \phi_0 = 1,\ \phi_1 = 1,\ \text{ at } \eta = 1 \end{array} \tag{3.10}$$

The analytical solutions of equations (3.4) to (3.9) with the boundary conditions in equation (3.10), are given by

$$\psi_0 = \lambda a_{13}[1 - \exp(-a_{10}\eta)] + a_{12}\eta + \frac{a_{16}\sinh a_{10}\eta}{\sinh a_{10}} + \frac{a_{11}\sinh a_1\eta}{\sinh a_1} \tag{3.11}$$

$$\psi_1 = \frac{a_{20}\sinh a_{17}\eta}{\sinh a_{17}} + \frac{a_{18}\sinh a_2\eta}{\sinh a_2} - \frac{a_{19}\sinh a_5\eta}{\sinh a_5} \tag{3.12}$$

$$\theta_0 = \frac{\sinh a_1\eta}{\sinh a_1} \tag{3.13}$$

$$\theta_1 = \frac{\sinh a_2\eta}{\sinh a_2} \tag{3.14}$$

$$\phi_0 = a_4\eta - \frac{a_3\sinh a_1\eta}{\sinh a_1} \tag{3.15}$$

$$\phi_1 = \frac{a_8\sinh a_5\eta}{\sinh a_5} - \frac{a_7\sinh a_2\eta}{\sinh a_2} \tag{3.16}$$

By substituting equations (3.11) to (3.16) into equations (3.1) to (3.3), we obtained solutions for the fluid velocity, temperature and concentration and are presented in the following form

$$\begin{aligned} \psi(\eta,\tau) = &\left[\lambda a_{13}[1 - \exp(-a_{10}\eta)] + a_{12}\eta + \frac{a_{16}\sinh a_{10}\eta}{\sinh a_{10}} + \frac{a_{11}\sinh a_1\eta}{\sinh a_1}\right] + \\ &\epsilon\ \exp(i\omega\tau)\left[\frac{a_{20}\sinh a_{17}\eta}{\sinh a_{17}} + \frac{a_{18}\sinh a_2\eta}{\sinh a_2} - \frac{a_{19}\sinh a_5\eta}{\sinh a_5}\right] \end{aligned} \tag{3.17}$$

$$\theta(\eta,\tau)=\left[\frac{\sinh a_1\eta}{\sinh a_1}\right]+\epsilon\ \exp(i\omega\tau)\left[\frac{\sinh a_2\eta}{\sinh a_2}\right] \tag{3.18}$$

$$\phi(\eta,\tau)=\left[a_4\eta-\frac{a_3\sinh a_1\eta}{\sinh a_1}\right]+\epsilon\ \exp(i\omega\tau)\left[\frac{a_8\sinh a_5\eta}{\sinh a_5}-\frac{a_7\sinh a_2\eta}{\sinh a_2}\right] \tag{3.19}$$

3.1 Skin friction : From the velocity field, the skin friction at the plate can be obtained, which is given in non dimensional form as

$$Cf=\left[\lambda a_{10}a_{13}\exp(-a_{10}\eta)+a_{12}+\frac{a_{10}a_{16}\cosh a_{10}\eta}{\sinh a_{10}}+\frac{a_1a_{11}\cosh a_1\eta}{\sinh a_1}\right]+$$
$$\epsilon\ \exp(i\omega\tau)\left[\frac{a_{17}a_{20}\cosh a_{17}\eta}{\sinh a_{17}}+\frac{a_2a_{18}\cosh a_2\eta}{\sinh a_2}-\frac{a_5a_{19}\cosh a_5\eta}{\sinh a_5}\right] \tag{3.20}$$

3.2 Nusselt number: From the temperature field, we obtained the heat transfer coefficient which is given in non-dimensional form as

$$Nu=-\left[\frac{a_1\cosh a_1\eta}{\sinh a_1}\right]-\epsilon\ \exp(i\omega\tau)\left[\frac{a_2\cosh a_2\eta}{\sinh a_2}\right]$$

3.3 Sherwood number: From the concentration field, we obtained the mass transfer coefficient which is given in non-dimensional form as

$$Sh=-\left[a_4-\frac{a_1a_3\cosh a_1\eta}{\sinh a_1}\right]-\epsilon\ \exp(i\omega\tau)\left[\frac{a_5a_8\cosh a_5\eta}{\sinh a_5}-\frac{a_2a_7\cosh a_2\eta}{\sinh a_2}\right] \tag{3.21}$$

4. RUSELTS AND DISCUSSION

A series of computations has been carried out for the effects of the following parameters: rotation parameter K^2, upper wall motion parameter λ, Hall current parameter m, thermal Grashof number Gr, solutal Grashof number Gm, magnetic parameter M, permeability parameter K, Prandtl number Pr, heat source parameter H, Schmidt number Sc and Soret number Sr on the fluid primary velocity U, secondary velocity W, temperature θ, concentration ϕ, skin friction Cf, Nusselt number Nu as well as Sherwood number Sh. In the present study following default parameter values are adopted for computations: $\tau=\pi/2$, $K^2=0.5$, $\lambda=0.1$, $Gr=2$, $Gm=4$, $M=m=K=Pr=H=Sr=\omega=1$, $Sc=0.22$ and $\varepsilon=0.5$. Therefore all the graphs and tables are corresponding to these values unless specifically indicated on the appropriate graph or table.

We notice that, from Fig. 2 the magnitude of the primary velocity component U reduces with an increase in rotation parameter K^2 whereas the secondary velocity component W enhances with an increase in rotation parameter K^2. This implies that rotation tends to retard the primary velocity whereas it has a reverse effect on the secondary velocity which is in agreement with the characteristics of Coriolis force which tends to suppress the primary flow for inducing the secondary flow.

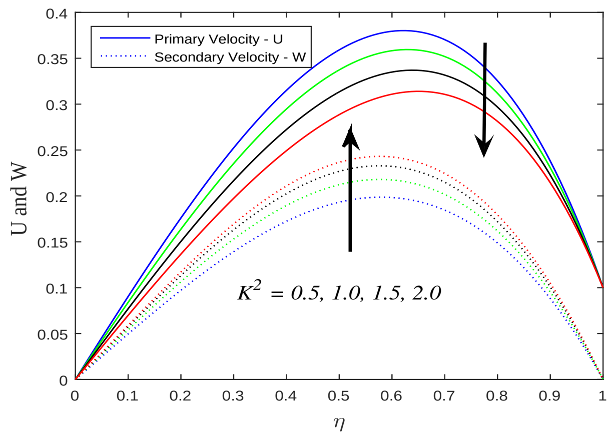

FIGURE 2. Influence of K^2 on fluid primary velocity and secondary velocity.

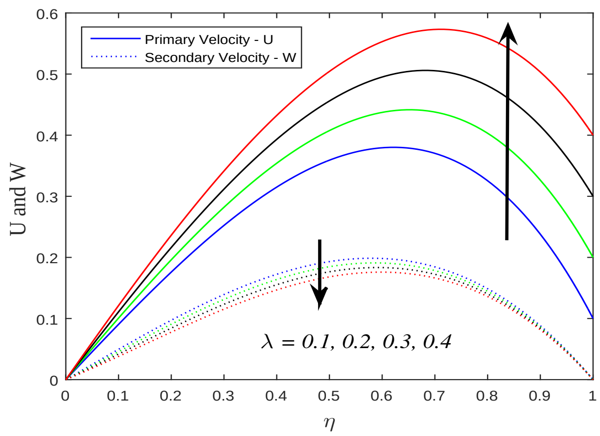

FIGURE 3. Influence of λ on fluid primary velocity and secondary velocity.

Fig. 3 depicts the influence of upper wall motion parameter λ. As λ is increasing, the fluid primary velocity U increases across the channel with maximum primary velocity at the upper wall and the fluid secondary velocity W decreases across the channel with minimum secondary velocity at the upper wall.The influence of the Hall current parameter m on primary velocity U and secondary velocity W is as shown in Fig.4. It is observed from these graphs that the primary velocity U and secondary velocity W increases with an increase in the Hall current parameter m.

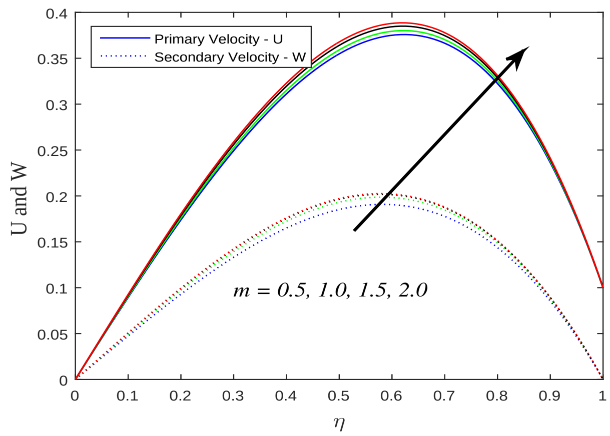

FIGURE 4. Influence of m on fluid primary velocity and secondary velocity.

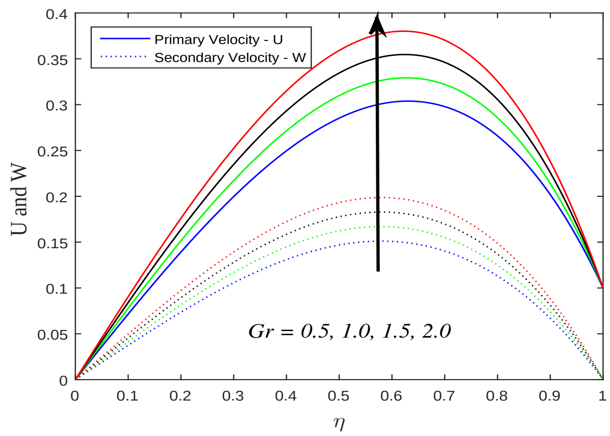

FIGURE 5. Influence of Gr on fluid primary velocity and secondary velocity.

The influence of Grashof numbers for heat and mass transfer are illustrated in Figs. 5 and 6 respectively on the fluid primary velocity U and secondary velocity W. The Grashof number Gr for heat transfer signifies the relative effect of the thermal buoyancy force to the viscous hydrodynamic force in the boundary layer. Grashof number Gm for mass transfer defines the ratio of the species buoyancy force to the viscous hydrodynamic force. It is observed that there

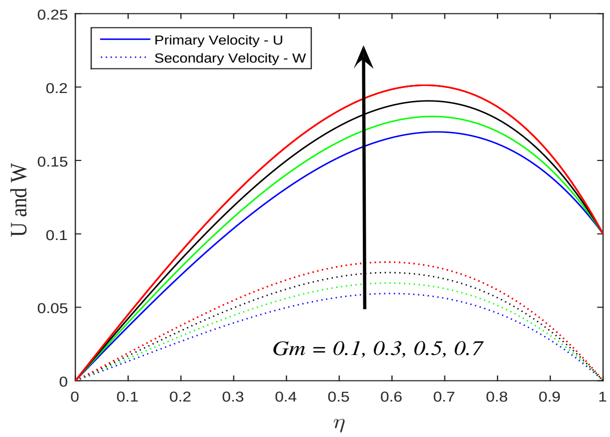

FIGURE 6. Influence of Gm on fluid primary velocity and secondary velocity.

was a rise in the primary velocity U and secondary velocity W due to the enhancement of thermal buoyancy force Gr and concentration buoyancy force Gm.

The influence of magnetic parameter M on the fluid primary velocity U and secondary velocity W is shown in the Fig. 7.

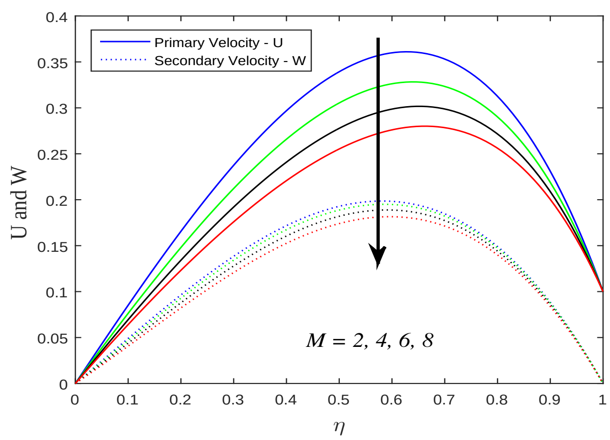

FIGURE 7. Influence of M on fluid primary velocity and secondary velocity.

it is noticed that, an increase in the magnetic parameter M decreases the fluid primary velocity U and secondary velocity W due to the resistive action of the Lorenz forces. This implies that magnetic field tends to decelerate fluid flow. Fig. 8 demonstrates the influence of permeability parameter K on the fluid primary velocity U and secondary velocity W. It is

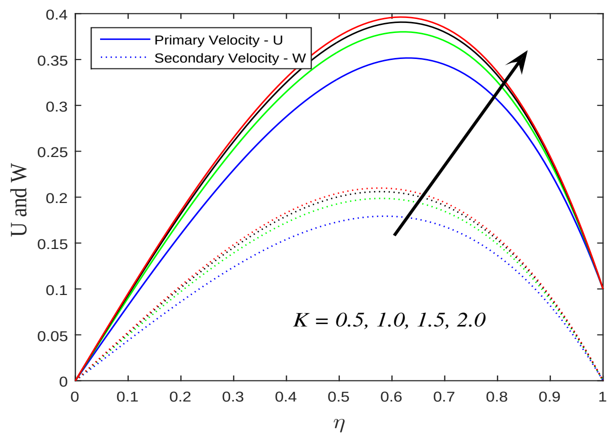

FIGURE 8. Influence of K on fluid primary velocity and secondary velocity.

observed that, the fluid primary velocity U and secondary velocity W increases on increasing the permeability parameter K.

Figs. 9 to 11, shows the plot of primary velocity U, secondary velocity W, temperature θ and concentration ϕ of the flow field against different values of Prandtl number Pr taking other parameters are constant. The Prandtl number defines the ratio of momentum diffusivity to thermal diffusivity. It is evident from Figs. 9 to 11, fluid primary velocity U, secondary velocity W and temperature θ decreases on increasing the Prandtl number Pr whereas concentration ϕ increases on increasing the Prandtl number Pr.

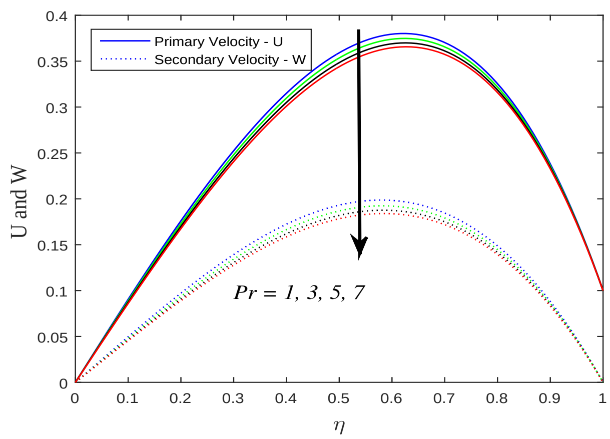

FIGURE 9. Influence of Pr on fluid primary velocity and secondary velocity.

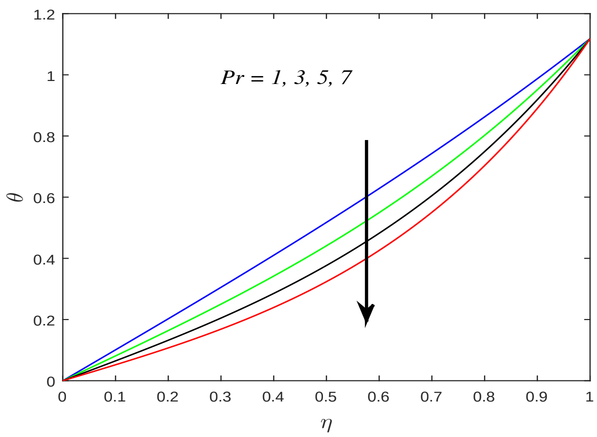

FIGURE 10. Influence of Pr on temperature.

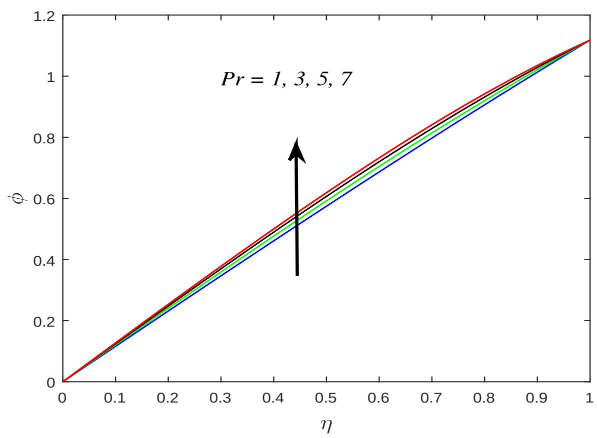

FIGURE 11. Influence of Pr on concentration.

Figs. 12 to 14, demonstrate the plot of fluid primary velocity U, secondary velocity W, temperature θ and concentration ϕ for a variety of heat source parameter H . It is seen in graphs that, the fluid primary velocity U, secondary velocity W and temperature θ decrease on increasing the heat source parameter H whereas concentration ϕ increases on increasing the heat source parameter H. This implies that heat source parameter reduced the fluid temperature.

The influence of fluid primary velocity U, secondary velocity W and concentration ϕ in presence of foreign species such as Hydrogen $(Sc = 0.22)$, Helium $(Sc = 0.30)$, Water vapour $(Sc = 0.60)$ and Ammonia $(Sc = 0.78)$ is shown in Figs.15 and 16.

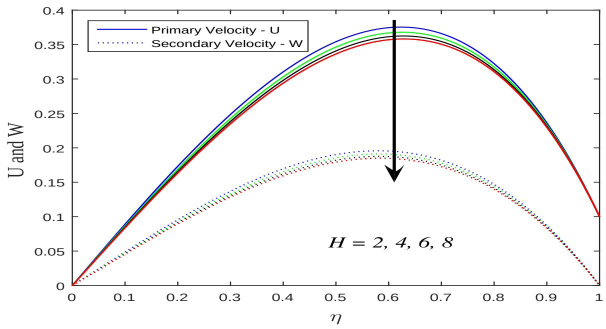

FIGURE 12. Influence of H on fluid primary velocity and secondary velocity.

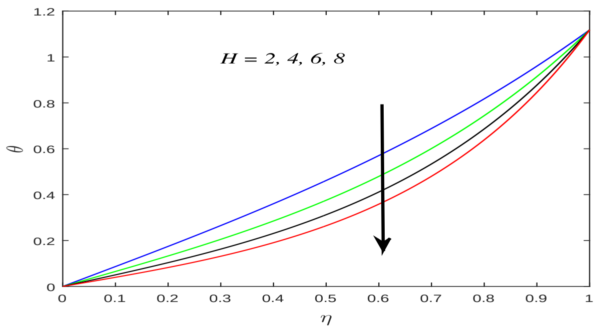

FIGURE 13. Influence of H on temperature.

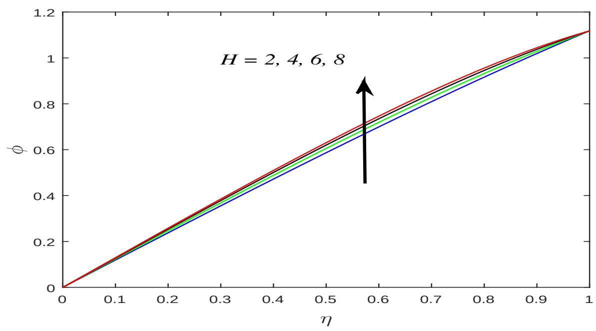

FIGURE 14. Influence of H on concentration.

Physically, Schmidt number signifies the relative strength of viscosity to chemical molecular diffusivity. It is noticed that, fluid primary velocity U, secondary velocity W and concentration ϕ increases on increasing the Schmidt number Sc.

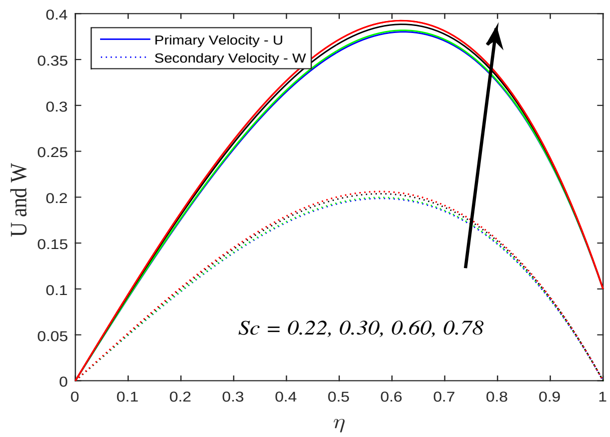

FIGURE 15. Influence of Sc on fluid primary velocity and secondary velocity.

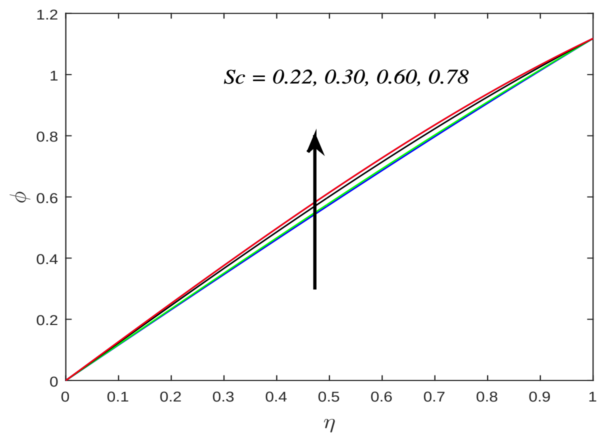

FIGURE 16. Influence of Sc on concentration.

Figs. 17 and 18 demonstrate the influence of Soret number Sr on the primary velocity U, secondary velocity W and species concentration ϕ. It is observed that, primary velocity U, secondary velocity W and species concentration ϕ increases on increasing the Soret number Sr. This implies that, Soret number tends to enhance the fluid primary velocity, secondary velocity and species concentration.

From tables 1 to 3, it is clear that the primary skin friction coefficient increases on increasing the upper wall motion parameter λ at both cold and heated plates.The primary skin friction

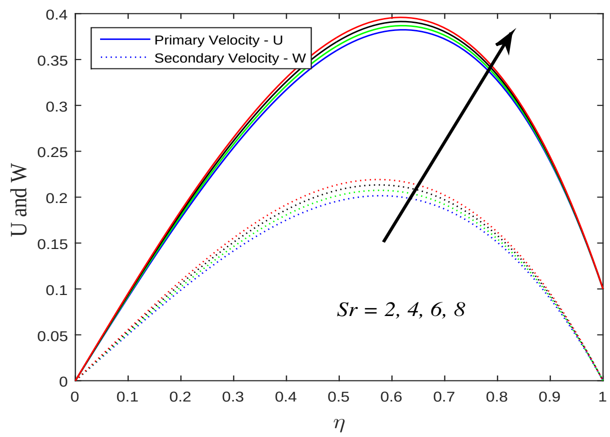

FIGURE 17. Influence of Sr on fluid primary velocity and secondary velocity.

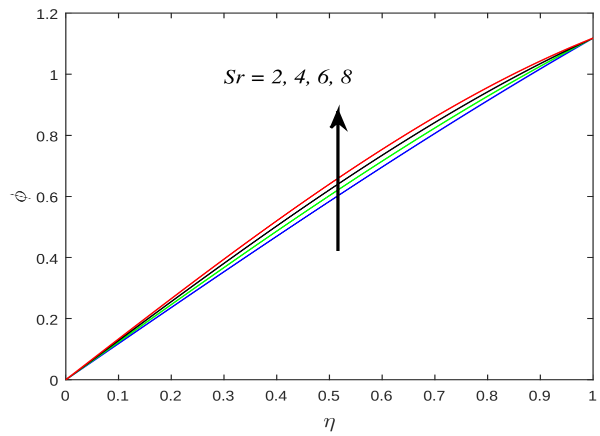

FIGURE 18. Influence of Sr on concentration.

coefficient decreases at the cold wall and increases at the heated wall on increasing the rotation parameter K^2, magnetic parameter M, Prandtl number Pr and heat source parameter H whereas it is increases at the cold wall and decreases at the heated wall on increasing the Hall current parameter m, thermal Grashof number Gr, solutal Grashof number Gm , permeability parameter K, Schmidt number Sc and Soret number Sr. The secondary skin friction coefficient decreases at the cold wall and increases at the heated wall on increasing the upper wall motion parameter λ, magnetic parameter M, Prandtl number Pr and heat source parameter H whereas it is increases at the cold wall and decreases at the heated wall on increasing the rotation parameter K^2, Hall current parameter m, thermal Grashof number Gr, solutal Grashof number Gm , permeability parameter K, Schmidt number Sc and Soret number Sr.

From table 4, it is clear that the heat transfer coefficient Nu increases at the cold wall, decreases at the heated wall on increasing the Prandtl number Pr, heat source parameter H.

From table 5, it is clear that the mass transfer coefficient Sh decreases at the cold wall and increases at the heated wall on increasing the Prandtl number Pr, heat source parameter H, Schmidt number Sc and Soret number Sr.

TABLE 1. Influence of K^2, m, λ and M on the skin friction coefficient.

K^2	m	λ	M	Skin friction coefficient			
				Primary		Secondary	
				Cold wall	Heated wall	Cold wall	Heated Wall
0.5	1.0	0.1	1.0	0.9135	-1.6594	0.4945	-1.0279
1.0	1.0	0.1	1.0	0.8490	-1.5848	0.5359	-1.1002
1.5	1.0	0.1	1.0	0.7784	-1.5029	0.5633	-1.1578
2.0	1.0	0.1	1.0	0.7057	-1.4178	0.5762	-1.2004
0.5	0.5	0.1	1.0	0.9051	-1.6427	0.4724	-0.9999
0.5	1.0	0.1	1.0	0.9135	-1.6594	0.4945	-1.0279
0.5	1.5	0.1	1.0	0.9253	-1.6776	0.5043	-1.0383
0.5	2.0	0.1	1.0	0.9347	-1.6910	0.5079	-1.0410
0.5	1.0	0.1	1.0	0.9135	-1.6594	0.4945	-1.0279
0.5	1.0	0.2	1.0	1.0185	-1.5394	0.4484	-1.0056
0.5	1.0	0.3	1.0	1.1234	-1.4194	0.4024	-0.9834
0.5	1.0	0.4	1.0	1.2284	-1.2995	0.3564	-0.9611
0.5	1.0	0.1	2.0	0.8625	-1.5882	0.4862	-1.0301
0.5	1.0	0.1	4.0	0.7776	-1.4637	0.4596	-1.0228
0.5	1.0	0.1	6.0	0.7123	-1.3598	0.4256	-1.0062
0.5	1.0	0.1	8.0	0.6627	-1.2726	0.3889	-0.9849

TABLE 2. Influence of K, Gr, Gm and Pr on the skin friction coefficient.

K	Gr	Gm	Pr	Skin friction coefficient			
				Primary		Secondary	
				Cold wall	Heated wall	Cold wall	Heated Wall
0.5	2.0	4.0	1.0	0.8289	-1.5443	0.4362	-0.9602
1.0	2.0	4.0	1.0	0.9135	-1.6594	0.4945	-1.0279
1.5	2.0	4.0	1.0	0.9451	-1.7014	0.5168	-1.0534
2.0	2.0	4.0	1.0	0.9616	-1.7232	0.5287	-1.0669
1.0	0.5	4.0	1.0	0.7227	-1.2278	0.3716	-0.7793
1.0	1.0	4.0	1.0	0.7863	-1.3717	0.4125	-0.8622
1.0	1.5	4.0	1.0	0.8499	-1.5155	0.4535	-0.9450
1.0	2.0	4.0	1.0	0.9135	-1.6594	0.4945	-1.0279
1.0	2.0	0.1	1.0	0.3732	-0.4856	0.1272	-0.3271
1.0	2.0	0.3	1.0	0.4009	-0.5458	0.1461	-0.3631
1.0	2.0	0.5	1.0	0.4286	-0.6060	0.1649	-0.3990
1.0	2.0	0.7	1.0	0.4563	-0.6662	0.1837	-0.4349
1.0	2.0	4.0	1.0	0.9135	-1.6594	0.4945	-1.0279
1.0	2.0	4.0	3.0	0.8969	-1.6398	0.4756	-1.0059
1.0	2.0	4.0	5.0	0.8819	-1.6219	0.4614	-0.9887
1.0	2.0	4.0	7.0	0.8690	-1.6061	0.4510	-0.9754

TABLE 3. Influence of H, Sc and Sr on the skin friction coefficient.

H	Sc	Sr	Skin friction coefficient			
			Primary		Secondary	
			Cold wall	Heated wall	Cold wall	Heated Wall
2.0	0.22	1.0	0.8989	-1.6420	0.4857	-1.0176
4.0	0.22	1.0	0.8766	-1.6144	0.4720	-1.0011
6.0	0.22	1.0	0.8604	-1.5933	0.4619	-0.9884
8.0	0.22	1.0	0.8482	-1.5766	0.4542	-0.9784
1.0	0.22	1.0	0.9135	-1.6594	0.4945	-1.0279
1.0	0.30	1.0	0.9188	-1.6656	0.4978	-1.0316
1.0	0.60	1.0	0.9390	-1.6891	0.5100	-1.0455
1.0	0.78	1.0	0.9515	-1.7035	0.5172	-1.0538
1.0	0.22	2.0	0.9205	-1.6676	0.5034	-1.0380
1.0	0.22	4.0	0.9344	-1.6838	0.5212	-1.0584
1.0	0.22	6.0	0.9484	-1.7001	0.5390	-1.0787
1.0	0.22	8.0	0.9623	-1.7164	0.5569	-1.0990

TABLE 4. Influence of Pr and H on the heat transfer coefficient.

Pr	H	Heat transfer coefficient	
		Cold wall	Heated wall
1.0	1.0	-1.0078	-1.3427
3.0	1.0	-0.8076	-1.7789
5.0	1.0	-0.6442	-2.1770
7.0	1.0	-0.5157	-2.5343
1.0	2.0	-0.8631	-1.6662
1.0	4.0	-0.6482	-2.2234
1.0	6.0	-0.4992	-2.6958
1.0	8.0	-0.3919	-3.1094

TABLE 5. Influence of H, Sc, Sr and Pr on the mass transfer coefficient.

H	Sc	Sr	Pr	Mass transfer coefficient	
				Cold wall	Heated wall
2.0	0.22	1.0	1.0	-1.1913	-0.9642
4.0	0.22	1.0	1.0	-1.2389	-0.8409
6.0	0.22	1.0	1.0	-1.2720	-0.7366
8.0	0.22	1.0	1.0	-1.2959	-0.6452
1.0	0.22	1.0	1.0	-1.1592	-1.0358
1.0	0.30	1.0	1.0	-1.1743	-1.0057
1.0	0.60	1.0	1.0	-1.2319	-0.8919
1.0	0.78	1.0	1.0	-1.2671	-0.8230
1.0	0.22	2.0	1.0	-1.1842	-0.9863
1.0	0.22	4.0	1.0	-1.2344	-0.8881
1.0	0.22	6.0	1.0	-1.2847	-0.7916
1.0	0.22	8.0	1.0	-1.3353	-0.6973
1.0	0.22	1.0	1.0	-1.1592	-1.0358
1.0	0.22	1.0	3.0	-1.2051	-0.9412
1.0	0.22	1.0	5.0	-1.2428	-0.8557
1.0	0.22	1.0	7.0	-1.2724	-0.7794

5. Conclusions

In this paper we have studied analytically the influence of hall current and heat source on unsteady MHD flow of a rotating fluid in a parallel porous plate channel. From the present investigation the following conclusions can be drawn:

- Primary velocity decreases and secondary velocity increases on increasing the rotation parameter. The primary skin friction coefficient decreases at the cold wall and increases at the heated wall whereas the secondary skin friction coefficient increases at the cold wall and decreases at the heated wall with an increase in the rotation parameter.
- Primary velocity increases and secondary velocity decreases on increasing the upper wall motion parameter. The primary skin friction coefficient increases at both cold and heated walls whereas the secondary skin friction coefficient decreases at the cold wall and increases at the heated wall with an increase in the upper wall motion parameter.
- Both the primary and secondary velocity profiles are increases on increasing the Hall current parameter and Soret number. Primary and secondary skin friction coefficients are increases at the cold wall and decreases at the heated wall on increasing the Hall current parameter and Soret number.
- The primary and secondary velocity profiles are decreases on increasing the heat source parameter. Primary and secondary skin friction coefficients are decreases at the cold wall and increases at the heated wall on increasing the heat source parameter.

Acknowledgments

The authors are extremely thankful to the learned referee for his valuable suggestions and comments towards the improvement of the paper.

Nomenclature

a – distance between two parallel plates	j_w – mass flux
B_0 – uniform magnetic field	K – non dimensional permeability parameter
C – species concentration	k_T – thermal conductivity of the fluid
C_f – skin-friction coefficient	K^2 – non dimensional rotation parameter
C_1 – species concentration at the heated wall	m – Hall current parameter
C_0 – species concentration at the cold wall	M – Magnetic parameter
c_p – specific heat at constant pressure	Nu – Nusselt number
K_1 – dimensional permeability parameter	n – dimensional frequency of oscillation
D_m – chemical molecular diffusivity	Pr – Prandtl number
Sr – Soret number	Q_0 – dimensional heat source parameter
p – fluid pressure	q_w – heat flux
Gm – Solutal Grashof number	Sc – Schmidt number
Gr – thermal Grashof number	Sh – Sherwood number
g – acceleration due to gravity	T – fluid temperature
H – non- dimensional heat source parameter	T_m – mean temperature of the fluid

T_1 – fluid temperature at the heated wall
T_0 – fluid temperature at the cold wall
t – dimensional time
U – primary velocity
W – secondary velocity
u – fluid velocity in x – direction
v – fluid velocity in y – direction
w – fluid velocity in z – direction

Greek Symbols

β_c – coefficient expansion for species concentration
β_T – coefficient of thermal expansion
ν – kinematic coefficient of viscosity
λ – upper wall motion parameter
ω – A scaled frequency
ϕ – A scaled concentration
ρ – fluid density
Ω – dimensional rotation parameter
σ – electrical conductivity
τ – non dimensional time
τ_w – shear stress
ψ – compact velocity
η – A scaled coordinate
θ – A scaled temperature

APPENDIX

$$a_1 = \sqrt{PrH}, a_2 = \sqrt{Pr(H+i\omega)}, a_3 = ScSr, a_4 = 1 + a_3, a_5 = \sqrt{Sci\omega},$$

$$a_6 = \frac{a_2^2}{a_2^2 - a_5^2}, a_7 = a_3 a_6, a_8 = 1 + a_7, a_9 = \frac{M}{1+im} - 2iK^2, a_{10} = \sqrt{a_9 + \frac{1}{K}},$$

$$a_{11} = \frac{Gma_3 - Gr}{a_1^2 - a_{10}^2}, a_{12} = \frac{Gma_4}{a_{10}^2}, a_{13} = \frac{a_9}{a_{10}^2}, a_{14} = \lambda - (a_{11} + a_{12}),$$

$$a_{15} = \lambda a_{13}[1 - exp(-a_{10})], a_{16} = a_{14} - a_{15}, a_{17} = \sqrt{a_9 + \frac{1}{K} + i\omega}, a_{18} = \frac{Gma_7 - Gr}{a_2^2 - a_{17}^2},$$

$$a_{19} = \frac{Gma_8}{a_5^2 - a_{17}^2}, a_{20} = a_{19} - a_{18}.$$

REFERENCES

[1] B. K. Sharma and R. C. Chaudhary: *Hydromagnetic unsteady mixed convection and mass transfer flow past a vertical porous plate immersed in a porous medium with Hall Effect*, Engineering Transactions, **56** (2008), pp. 3 –23.

[2] A. M. Salem and M. Abd El-Aziz: *Effect of hall currents and chemical reaction on hydromagnetic flow of a stretching vertical surface with internal heat generation or absorption*, Applied Mathematical Modeling, **32** (2008), pp. 1236 – 1254.

[3] M. Venkateswarlu and D. Venkata Lakshmi: *Dufour and chemical reaction effects on unsteady MHD flow of a viscous fluid in a parallel porous plate channel under the influence of slip condition*, Journal of the Nigerian Mathematical Society, **36** (2017), pp. 369 – 397.

[4] M. Turkyilmazoglu: *Exact solutions for the incompressible viscous magnetohydrodynamic fluid of a porous rotating disk flow with hall current*, Int. J. Mech. Sci. **56** (2012), pp. 86 – 95.

[5] A. A. Khan, F. Masood, R. Ellahi and M. M. Bhatti: *Mass transport on chemicalized fourth-grade fluid propagating peristaltically through a curved channel with magnetic effects*, Journal of Molecular Liquids, **258** (2018), pp. 186 – 195.

[6] R. Ellahi, M. M. Bhatti and I. Pop: *Effects of hall and ion slip on MHD peristaltic flow of Jeffrey fluid in a non-uniform rectangular duct*, International Journal of Numerical Methods for Heat and Fluid Flow, **26** (2016), pp. 1802 – 1820.

[7] M. Venkateswarlu and D. Venkata Lakshmi: *Thermal diffusion, hall current and chemical reaction effects on unsteady MHD natural convective flow past a vertical plate*, U. P. B. Sci. Bull., Series D: Mechanical Engineering, **79** (2017), pp. 91 – 106.

[8] S. Sarkar and G. S. Seth: *Unsteady hydromagnetic natural convection flow past a vertical plate with time-dependent free stream through a porous medium in the presence of Hall current, rotation and heat absorption*, Journal of Aerospace Engineering, **30** (2017), pp. 04016081 – 1 – 11.

[9] D. Tripathi, T. Hayat, N. Ali, and S. K. Pandey: *Effects of transverse magnetic field on the peristaltic transport of viscoelastic fluid with Jeffrey model in a finite length channel*, International Journal of Modern Physics b, **25** (2011), pp. 3455 – 3471.

[10] B. K. Jha, C. A. Apere: *Hall and ion-slip on unsteady MHD Couette flow in a rotating system with suction and injection*, J. Phys. Soc. Jpn. **80** (2011), pp. 114401.

[11] M. Venkateswarlu, G. V. Ramana Reddy and D. V. Lakshmi:*Effects of chemical reaction and heat generation on MHD boundary layer flow of a moving vertical plate with suction and dissipation*, Engineering International, **1** (2013), pp. 27 – 38.

[12] B. K. Jha and M. O. Oni: *Electromagnetic natural convection flow in a vertical micro-channel with joule heating: Exact solution*, J Taibah Univ Sci. **12** (2018), pp. 661 – 668.

[13] M. Venkateswarlu, G. V. Ramana Reddy and D. V. Lakshmi: *Diffusion-thermo effects on MHD flow past an infinite vertical porous plate in the presence of radiation and chemical reaction*, International Journal of Mathematical Archive, **4** (2013), pp. 39 – 51.

[14] M. M. Bhatti, A. Zeeshan, R. Ellahi and G. C. Shit: *Mathematical modeling of heat and mass transfer effects on MHD peristaltic propulsion of two-phase flow through a Darcy-Brinkman-Forchheimer porous medium*, Advanced Powder Technology, **29** (2018), pp. 1189 – 1197.

[15] R. Ellahi, M. Khan, A. S. Nehad: *Combine porous and magnetic effect on some fundamental motions of Newtonian fluids over an infinite plate*, J. Porous Media, **21** (2018), pp. 589 – 605.

[16] M. Venkateswarlu and O. D. Makinde: *Unsteady MHD slip flow with radiative heat and mass transfer over an inclined plate embedded in a porous medium*, Defect and Diffusion Forum, **384** (2018), pp. 31 – 48.

[17] S. Das, H. K. Mandal and R. N. Jana: *Hall effects on unsteady rotating MHD flow through porous channel with variable pressure gradient*, International Journal of Computer Application, **83** (2013), pp. 7 – 18.

[18] M. Venkateswarlu, D. Venkata Lakshmi and G. Darmaiah: *Influence of slip condition on radiative MHD flow of a viscous fluid in a parallel porous plate channel in presence of heat absorption and chemical reaction* , J. Korean Soc. Ind. Appl. Math, **20** (2016), pp. 333 – 354.

[19] M. Venkateswarlu, R. Vasu Babu and S. K. Mohiddin Shaw: *Dufour and heat source effects on radiative MHD slip flow of a viscous fluid in a parallel porous plate channel in presence of chemical reaction*, J. Korean Soc. Ind. Appl. Math, **21** (2017), pp. 245 –275.

[20] M. Venkateswarlu and M. Phani kumar: *Soret and heat source effects on MHD flow of a viscous fluid in a parallel porous plate channel in presence of slip condition*, U. P. B. Sci. Bull., Series D: Mechanical Engineering, **79** (2017), pp. 171 – 186.

[21] O. D. Makinde, Adetayo S. Eegunjobi and M. Samuel Tshehla: *Thermodynamics analysis of variable viscosity hydromagnetic couette flow in a rotating system with Hall effects*, Entropy, **7** (2015), pp. 7811 – 7826.

[22] S. O. Adesanya and O. D. Makinde: *MHD oscillatory slip flow and heat transfer in a channel filled with porous media*, U. P. B. Sci. Bull. Series A, **76** (2014), pp. 197 – 204.

[23] M. Venkateswarlu and D. Venkata Lakshmi: *Soret and chemical reaction effects on the radiative MHD flow from an infinite vertical plate*, J. Korean Soc. Ind. Appl. Math, **21** (2017), pp.39 – 61.